치의과학박사 학위논문

Preclinical comparison study of single- and double-root 3D-printed Ti-6Al-4V implant

Ti-6Al-4V로 제작한 단근 및 다근 3D-프린트 임플란트의 전임상 비교연구

2023년 8월

서울대학교 대학원

치의과학과 치주과학 전공

정 인 나

Preclinical comparison study of single- and double-root 3D-printed Ti-6Al-4V implant

지도교수 구 기 태

이 논문을 치의과학박사 학위논문으로 제출함
2023년 5월

서울대학교 대학원
치의과학 치주과학 전공
정 인 나

정인나의 치의과학박사 학위논문을 인준함
2023년 7월

위 원 장 _____ (인)

부위원장 _____ (인)

위 원 _____ (인)

위 원 _____ (인)

위 원 _____ (인)

Abstract

Preclinical comparison study of single- and double-root 3D-printed Ti-6Al-4V implant

Inna Chung, D.D.S., M.S.D.

Program in Periodontology

Department of Dental Science

Graduate School, Seoul National University

(Directed by Prof. Ki-Tae Koo, D.D.S., M.S.D., Ph.D.)

Objectives. Recently, double-root implants have been investigated using 3D-printed technology. The purpose of this study was to compare the stability of single- and double-root 3D-printed implants. The secondary aim was to compare single- and double-root 3D-printed implants in micro-computed tomographic(micro-CT) and histological analyses.

Materials and Methods. Single- and double- root 3D-printed implants were fabricated and placed at mandibular third and fourth premolars in four beagle dogs. Eight implants in each group were placed immediately after tooth extraction. Damping capacity was measured, and periapical X-rays were taken every 2 weeks for 12 weeks. Bone volume/tissue volume (BV/TV) and bone mineral density (BMD) around the implants were measured with micro-computed tomography. Bone-to-implant contact (BIC) and bone area fraction occupancy (BAFO) were measured in histological samples.

Results. All single- and double-root 3D implants survived without clinical signs of peri-implant inflammation. The implant stability values between the groups were not statistically different, except at 4 and 12 weeks. The marginal bone changes were observed to be not statistically different in mesial and distal areas between the groups, except in the middle site of double-root implants. The BV/TV and BMD of double-root 3D-printed implants showed no statistically significant difference in micro-CT analyses, but less BIC and BAFO values in histomorphometric analyses compared to single-root 3D-printed implants.

Conclusion. Compared to single-root implants, 3D-printed double-root implants demonstrated comparable stability and bone remodeling around the fixture, but statistically significant marginal bone loss in the furcation area remains problematic.

Keywords: Dental implant, Osseointegration, 3D printing

Student Number: 2020-39210

Table of Contents

Preclinical comparison study of single- and double-root 3D-printed Ti-6Al-4V implant

Inna Chung, D.D.S., M.S.D.

Program in Periodontology

Department of Dental Science

Graduate School, Seoul National University

(Directed by Prof. Ki-Tae Koo, D.D.S., M.S.D., Ph.D.)

I. Introduction

With the recent increase in the elderly population, those in need of dental rehabilitation in edentulous areas are also increasing [1]. Research on implant designs, materials, and techniques has been flourishing in recent decades, and such advances have led to an implant survival rate of approximately 95% according to 10-year clinical observations [2-5]. From this evidence, dental implants are considered an ideal option for functionally and aesthetically restoring missing tooth areas. However, conventional dental implants are not entirely consistent with patient-specific treatment strategies, necessitating additional surgical procedures, such as drilling or bone grafting.

Various efforts have been made to implement root analog implants to provide patient-specific dental treatment. The first attempt to apply a patient-specific root analog implant was made by Hodosh et al. in 1969 [6]. They reported that collagenous fibers of the periodontal ligament were inserted into the implant; however, when interpreted based on current histological knowledge, osseointegration failed and was considered to be fibrointegrated [7]. As the material was changed from polymethacrylate to titanium, root-analog implant fabrication became possible, and numerous

studies reported successful preclinical and clinical outcomes of root-analog implants [7-14].

With the advance of digital technologies and materials, elaborate 3D-printed personalized implant fabrication has become possible [15–17]. By virtue of the development of cone beam computed tomography (CT), oral scanning, and computer-aided design software, personalized 3D-printed implant structures can be manipulated and subsequently fabricated with additive manufacturing. A great number of studies have reported on 3D-printed implants displaying successful osseointegration and good biocompatibility in vivo [18-20]. In terms of the material, the sand-blasted 3D-printed Ti-6Al-4V specimen had similar biological properties in terms of adherent cell numbers, vinculin intensity, osteogenic gene expression, and biomineralization to those of the machine-cut counterpart, indicating the potential usefulness of 3D printing technology in dental implants [21]. Elastic modulus of commercially pure titanium is 112 GPa, whereas the titanium alloy Ti-6Al-4V, 115 GPa, and both display similar morphology, topography, phase composition and chemistry, and osseointegration and biomechanical anchorage [22-24]. In vitro studies of 3D-printed Ti-6Al-4V implants also revealed no harmful or adverse effects on cell proliferation or spread, indicating

that it is biocompatible [25–28]. As expected, the micro- and nano-structured implants outperformed the polished implants in terms of osteogenic differentiation at both the protein and gene levels [20]. In addition, Shaoki et al. demonstrated that 3D-printed implants had similar bone volume/tissue volume (BV/TV) values and bone to implant contact (BIC) ratios to machined implants, even though cell adhesion, osteoblast differentiation, and removal torque were higher on the former [29]. 3D-printed implants with double roots in the posterior region have been suggested as an alternative to alleviate the mechanical complications of conventional implants and regenerative procedures [30].

Recently, we investigated 3D-printed double-root implants designed under a digital workflow with digital data and software, and fabricated with a direct metal laser sintering machine using Ti-6Al-4V powder in vivo [29]. In this study, we found that the macrodesign of a 3D-printed implant with a groove has a significant positive effect on secondary implant stability [29]. A peculiarity was found in that the marginal bone changes in the furcation area were larger than those in the mesial or distal areas for lattice-type 3D-printed implants [29]. As it is difficult to perform daily self-cleansing of furcation-involved teeth, bacterial accumulation progresses continuously, and the long-term prognosis of the teeth

cannot be guaranteed [25]. Therefore, before implementing double-root implants in clinical situations, it is necessary to investigate the outcome of furcation-involved double-root implants and examine whether periodontal healthy conditions can be secured compared with single-root implants.

Therefore, the purpose of this study is to investigate the marginal bone changes of double-root 3D-printed implants using Ti-6Al-4V powder compared to single-root 3D-printed implants, in addition to implant stability and micro-computed tomography (micro-CT) and histological analyses.

II. Materials and Methods

1. Animals

All methods in this animal experiment were performed in conformity with the principles of the 3R (replacement, reduction, and refinement) and two major laws in Korea, which are the Animal Protection Act established by the Ministry of Agriculture, Food, and Rural Affairs and the Laboratory Animal Act established by the Ministry of Food and Drug Safety. The animal experiment was evaluated and authorized by the Institutional Animal Care and Use Committee of Seoul National University (IACUC; approval no. SNU-210115-1) and performed in accordance with the Animal Research: Reporting of In Vivo Experiments (ARRIVE) guidelines. The study comprised four 1-year-old male beagle dogs, weighing approximately 10–12 kg. The manuscript was written in compliance with the ARRIVE guidelines.

2. Surgical procedures

Fabrication of 3D-printed implants

The fabrication process of the 3D-printed implants was conducted according to a previous study [31]. CT datasets of the

mandible were obtained using a CT scanner (GE, Boston, USA) and imported into 3D reconstruction software (Materialise, Leuven, Belgium) via the Digital Imaging and Communications in Medicine format. Right and left mandibular third and fourth premolars were virtually extracted and isolated as a stereolithography (STL) file with the software. The STL file was transferred into software (Materialise) to fabricate 3D single-root implants at the distal root of the third premolar area and double-root implants at the fourth premolar area with a direct metal laser sintering machine using Ti-6Al-4V powder through Dentium Build Processor 1.4.7 (Dentium, Seoul, Korea) powered by KETI Slicing Engine. The single-root implant and mesial root of the double-root implants were manufactured to be 2 mm longer than the corresponding teeth with a groove to obtain primary stability. The implants were marked with numbers and letters in the upper area to denote animals and locations (Figure 1). The root dimensions of the 3D-printed implants were different for each tooth, but the abutment was manufactured with a constant size (Figure 1). Following large-grit sandblasting and acid-etching (SLA) surface treatment according to a previous study, the 3D-printed implants were sterilized using gamma-ray irradiation, which emits short-wavelength light from a cobalt-60 (60Co) radioactive isotope. A surgical guide and drills to

perform osteotomies at the mesial roots of the planned sites were fabricated through a digital light processing (DLP) 3D-printer (Dental 3DPrinter-P, Dentium, Seoul, Korea) using the material Surgical Guide (DG-1). The protective cap was fabricated with polymer with a thickness of 1 mm to minimize loading on the implant (DG-1, Hephzibah, Inchon, Korea) (Figure 1).

Immediate placement of 3D-printed implants

The animals were anesthetized by a veterinarian using intravenous injections of tiletamine/zolazepam (5 mg/kg, Virbac, Carros, France), xylazine (2.3 mg/kg, Bayer Korea, Ansan, Korea), and 0.05 mg/kg atropine sulfate for the surgery. Complementary local anesthesia was injected at the mandibular third and fourth premolar areas with 2% lidocaine HCl and epinephrine (1:1,000,000, Huons, Seongnam, Korea). The third and fourth premolars were hemisectioned with a diamond fissure bur in the buccolingual direction of the teeth and atraumatically extracted with elevator and forceps without flap reflection. The apical portion of the extraction socket was prepared using a 2.3-mm drill with a motor-driven handpiece (EXPERTsurg LUX, KaVo, Warthausen, Germany) to be 2 mm longer than the corresponding root for a single-root 3D-printed implant and the mesial root for a double-root 3D-printed

implant. The 3D-printed implant heads were directly tapped using a surgical mallet. The protective cap was attached to the adjacent teeth using resin-modified glass ionomer cement (GC FujiCEM2, Tokyo, Japan).

Postoperative care

An antibiotic (cefazoline, 20 mg/kg, Chongkundang Pharm., Seoul, Korea) and analgesic (tramadol hydrochloride, 5 mg/kg, Samsung Pharm., Hwaseong, Korea) were intravenously injected after surgery to relieve postoperative pain and inflammation. For 3 days after the surgery, antibiotics and analgesics were administered by mixing them with the animals' diet. To prevent any mechanical pressure that might hinder wound healing, a soft diet was provided for a month. The surgical sites were inspected every 2 weeks and rinsed with a 0.12% chlorhexidine gluconate solution (Hexamedine, Bukwang Pharm., Seoul, Korea).

3. Implant stability measurements

Based on a previous study [16, 21, 23], damping capacity analysis (Anycheck, Neobiotech, Seoul, Korea) was performed at implant placement and every two weeks following until 12 weeks to measure implant stability. Measurements were taken five times

from the buccal side of each implant, and the average value was considered representative.

4. Marginal bone changes

The marginal bone level was measured with periapical radiographs taken at implant placement, 6 and 12 weeks after implant placement. The measurement was performed at the mesial and distal sites of each implant and at the middle sites in the case of double-root implants. The proportion between the actual distance and the distance on the radiograph was calculated. In the radiographs taken at implant placement, 6 weeks, and 12 weeks after implant placement, the distance between the alveolar crest and implant platform was measured on the radiograph and converted to the actual distance between the alveolar crest and implant platform by applying the proportion. Mesial and distal marginal bone loss at 6 and 12 weeks were compared between the two 3D-printed implant groups. The marginal bone loss of the double-root 3D-printed implants at 6 and 12 weeks was compared among mesial, middle, and distal sites.

5. Micro-CT analyses

Animals were sacrificed 12 weeks after implant placement with potassium chloride (75 mg/kg, Jeil Pharm., Daegu, Korea). The block biopsy from each experimental site was harvested for micro-CT and histological preparation. The scan was performed at an energy of 60 kV, an intensity of 167 μA and a resolution of 13.3 μm using a 0.5-mm aluminum filter and a 3-dimensional micro-CT machine (SkyScan 1172, SkyScan, Aartselaar, Belgium). The data was reconstructed with the manufacturer's software (DataViewer 1.5.2.4 64-bit version, Bruker micro-CT, Skyscan, Kontich, Belgium) and quantitatively analyzed with CTAn (Bruker-CT, Kontich, Belgium). Based on a previous study [16], the volume of interest (VOI) was set to a 190 μm circular band stretching 60-2,250μm from the implant surface of each root, limiting 1 mm to 4 mm above the fixture apex. Within the VOI, bone mineral density (BMD) and BV/TV were measured using CTAn. The 8-bit grayscale values were set to range from 30 to 80 in order to identify bone tissue.

6. Histological preparation

After 1 week in a fixative solution containing 10% neutral

formalin buffer, the tissue sections were dehydrated in a series of ethanol solutions. Subsequently, the samples were embedded in methacrylate (Technovit 7200, Heraeus Kulzer, Hanau, Germany). The central mesiodistal sections were prepared and polished to approximately 45±5 μm and stained with Goldner trichrome.

7. Histological and histomorphometric analyses

Histological slides were stored as digital images after scanning with Panoramic 250 Flash III (3DHISTECH, Budapest, Hungary). The region of interest (ROI) was selected from 1 mm to 4 mm above the fixture apex using a computer-aided slide image analysis program (CaseViewer 2.2; 3DHISTECH Ltd., Budapest, Hungary). As described in a previous study [16], BIC and bone area fraction occupancy (BAFO) were measured on each 3D printed implant.

8. Statistical analysis

A sample size calculation was not performed due to the pilot nature of the study. All data for the two types of 3D-printed implants are presented as means ± SDs. A two-way ANOVA (implant type and time period) was conducted, and Sidak's double comparison test was performed for implant stability and marginal

bone changes. An unpaired t-test was conducted in the micro-CT analysis. Due to the lack of normality test passes, the Mann-Whitney test was performed for BIC and BAFO.

III. Results

1. Clinical observations

All single- and double-root implants survived (Figure 2). There were no clinical signs of peri-implant inflammation, including redness, spontaneous bleeding, swelling, or ulceration.

2. Implant stability measurements

Implant stability values are presented in Figure 3. The implant stability value of single-root 3D-printed implants was 72.53±3.38 at the time of implant surgery and 70.83±3.63, 70.60±0.89, 71.73±4.16, 73.73±2.79, 72.93±2.04, and 72.60±1.46 at every 2 weeks after until 12 weeks following implant placement. The implant stability value of double-root 3D-printed implants was 75.71±2.03 at implant placement and 73.97±3.24, 72.92±1.65, 74.51±1.81, 73.65±1.80, 74.20±2.15, 75.54±0.96 at 2 weeks and 12 weeks following implant placement. There were no significant differences within the group at each time point, but statistically significant differences were observed between single- and double-root implants at 4 and 12 weeks ($p=0.0143$ and 0.0320).

3. Marginal bone changes

The marginal bone losses at the mesial sites of the single- and double-root 3D-printed implants were 0.85±0.45 mm and 1.06±0.95 mm, respectively, at 6 weeks. These values were 1.17±1.00 mm and 1.24±1.30 mm, respectively, at 12 weeks. No significant differences were observed in terms of the implant type or time point (Figure 4a). The marginal bone losses at the distal sites of the single- and double-root 3D-printed implants were 1.33±0.94 mm and 1.30±0.99 mm at 6 weeks, respectively. The values were 1.70±1.68 mm and 1.42±0.99 mm at 12 weeks. No significant differences were observed in terms of implant type or time point (Figure 4b).

The marginal bone losses at the middle site of the double-root 3D-printed implants at 6 weeks and 12 weeks were 2.55±0.50 mm and 3.00±0.85 mm, respectively. The marginal bone loss at the middle site of the double-root 3D-printed implant at each time point showed higher values than that at the mesial and distal sites of the double-root 3D-printed implant (Figure 4c).

4. Micro-CT analyses

The results from the micro-CT analysis are described in

Figure 5. The BV/TV values of the single-root and double-root 3D-printed implants were 67.11±13.05% and 60.76±5.43%, respectively, showing no statistically significant difference. The BMDs of the single-root and double-root 3D-printed implants were 1.11±0.23 $g \cdot mm^{-3}$ and 1.02±0.08 $g \cdot mm^{-3}$, respectively, showing no statistically significant difference.

5. Histological observations

All eight single-root and eight double-root 3D-printed implants survived. There were no specific signs of inflammation. Marginal bone loss at the mesial and distal sites was observed in both groups with no significant differences. A marginal bone loss pattern at the furcation area was observed for the double-root 3D-printed implants.

6. Histomorphometric analyses

The results from the micro-CT analysis are described in Figure 6. The BIC values for the single-root and double-root 3D-printed implants were significantly different (75.87%±6.32% and 64.18±5.23%, respectively, p=0.0070). The BAFO values were significantly different (p=0.0104) for the single-root and double-

root 3D-printed implants (64.88±14.37% and 45.81±9.01%, respectively).

IV. Discussion

This study compared the implant stability, marginal bone loss, BV/TV, BMD, BIC, and BAFO values of single- and double-root 3D-printed implants using Ti-6Al-4V powder through micro-CT, histological, and histomorphometric analyses. The double-root 3D-printed implants showed (i) greater implant stability, which was statistically significant at 4 and 12 weeks; (ii) comparable marginal bone loss in the proximal area but statistically greater marginal bone loss in the middle area; (iii) no significantly different BV/TV and BMD values through micro-CT analyses; and (iv) significantly lower BIC and BAFO values through histomorphometric analyses compared to single-root 3D-printed implants.

The conventional Ti-6Al-4V manufacturing technique relies on forging, casting, and rolling bulk raw materials, followed by subsequent machining to final forms and dimensions; however, these processes invariably produce significant material waste, high manufacturing costs, and protracted lead times [33-35]. In such cases, additive manufacturing (AM), a modern 3D printing technique that creates near-net-form structures directly from CAD models by adding materials layer-by-layer, offers its advantageous capability for the production of Ti-6Al-4V products with geometric

complexity [35-37]. Therefore, due to its free design, single-piece customization, and great process efficiency, it has met the urgent needs of the biomedical field in recent years [20].

The feasibility of individualized 3D-printed implants using the additive manufacturing method has been studied in merge with specific features such as macrodesign adjustments and surface treatments [9,13,14,17-19,21,24,25,31]. However, the evidence of the pros and cons of double-root 3D-printed implants in comparison to single-root 3D-printed implants is limited. This study found that double-root 3D-printed implants have comparable implant stability but greater marginal bone loss due to the furcation area compared to single-root 3D-printed implants.

The implant stability values at 4 and 12 weeks of the double-root implants showed higher values compared with those of the single-root implants. Most implant stability values were above 70, indicating that the implant was clinically stable for functional loading. The positive results of the two groups at all time points might stem from their groove structure, which resulted in high implant survival and stability as a macroretention structure for lattice-type 3D-printed implants in a previous study [31]. The values tended to be reduced at 2 and 4 weeks for each group, although that was not statistically significant within the groups. This tendency reflects the

stability dip, which results in the lowest implant stability value during the early healing period, as reported in several studies [24–26]. As in previous studies, the difference in the implant stability value according to implant structure, resulting in different surface area and diameter, appears to be most evident at the time of this stability dip [24,26]. In addition to the surface characteristics, the higher stability values at 4 weeks may be the result of the additional effect of the structural stability and the larger surface area of the double-root implant. The effect of a larger surface area on the stability value should be evaluated further in future studies.

In radiographic assessments, the single- and double-root 3D-printed implants displayed similar marginal bone loss values at mesial and distal sites regardless of the implant type and time point. For the double-root 3D-printed implants, significantly higher marginal bone loss was observed at the furcation area (middle) at each time point. This result can be explained by previous studies showing that a narrow inter-implant distance resulted in a greater probability of marginal bone loss [29,30]. In our study, the inter-root distance was narrow in the upper area because the 3D-printed implants reflected the shape of the teeth as much as possible with their tapered morphology. Taken together, these findings show that a narrow inter-root space in the upper area seems to result in

marginal bone loss in the furcation area.

According to the accepted standards for assessing implant survival and success, the vertical distance of marginal bone level change should be less than 2 mm from the expected marginal bone level following remodeling post-implant placement [31]. The systematic review and meta-analysis by Ragucci et al. evaluated the marginal bone loss in the implants placed immediately in the extraction socket in the molar areas, including data on 372 implants in 11 studies [32]. The marginal bone loss was estimated to be 1.29 ± 0.24 mm over the 1-year follow-up period, with a 95% CI of 0.81–1.76. Although differences in the study design, study subject, and implant material exist, the marginal bone loss found in the single-root 3D-printed implants of the current study (1.17±1.00 mm in mesial and 1.24±1.30 mm in distal area) is comparable to that of the previous studies. The marginal bone loss in the double-root 3D-printed implants showed comparable marginal bone loss values at the mesial and distal sites at 12 weeks (1.24±1.30 mm and 1.42±0.99 mm, respectively), but the value was statistically significantly greater at the middle site (3.00±0.85 mm).

In micro-CT analyses, the BV/TV and BMD values of the single-root and double-root 3D-printed implants did not differ significantly. Therefore, the quantity and density of the bone around

the 3D-printed implants appear to be unaffected by the number of roots. The morphology of the implant fixture does not seem to affect peri-implant bone healing when an implant with the proper surface for osseointegration is kept stable. These results corroborate that Ti-6Al-4V powder is a biocompatible material that is suitable for dental 3D-printed implants. This outcome is in line with our previous study, in which implants fabricated with the same materials showed comparable BV/TV and BMD values [24].

In histomorphometric analyses, the BIC and BAFO values were statistically lower for the double-root 3D-printed implants than for the single-root 3D-printed implants. This can probably be explained by the pattern in which the furcation area of the double-root implants exhibited significant interradicular bone resorption. Since BIC and BAFO refer to the amount or percentage of implant surface area in contact with the bone, the values are inevitably lower than those of single-root implants, which do not have the disadvantage of furcation. Implant design with double roots in the posterior regions has been suggested to reduce the mechanical complications of conventional implants; however, the outcome in furcation-involved areas remains enigmatic.

The limitation of this study was that the 3D-printed implants were analyzed only in the surgical stage, before prosthesis, and not

under prosthetic loading conditions. However, occlusion is one of the most significant factors affecting peri-implant hard tissue and implant success. In response to mechanical stress, occlusion can impact peri-implant hard tissue remodeling. From this perspective, future studies should incorporate comprehensive conditions to evaluate functional stability.

Another limitation of this study is the method of implant installation due to the shape of the double-root implants. The double-root 3D-printed implant has been incorporated to alleviate the mechanical complications of conventional implants and regenerative procedures, but the method of tapping the divergent double-root implant using a surgical mallet may increase strain within the bone. Although divergent roots distribute the occlusal force, the nature of the divergent root shape is a hindrance when placing the fixture into the bone. In addition, this process of placing the implant hinders the accurate positioning of the fixture apicocoronally and buccolingually since the tapping vector and force cannot be precisely controlled. Further studies should investigate the effect of striking 3D implant fixtures into the alveolar bone and possible errors derived from the process.

Within the limitations of this preclinical study, 3D-printed double-root implants had comparable stability, proximal marginal

bone loss, BV/TV, and BMD values compared with 3D-printed single-root implants. However, the double-root implants demonstrated significant marginal bone loss in the furcation area, which remains problematic.

V. Conclusion

Compared to single-root implants, 3D-printed double-root implants demonstrated comparable stability and bone remodeling around the fixture, but statistically significant marginal bone loss in the furcation area remains problematic.

VI. Table and figures

Figure 1. Computer-Aided Design (CAD) images of 3D-printed implants and protective caps

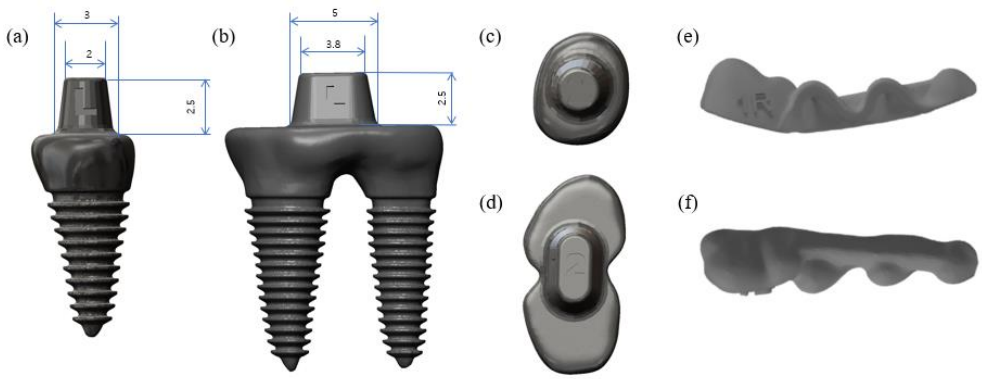

Computer-Aided Design (CAD) images of 3D-printed implants and protective caps (a) Side view of a single-root 3D-printed implant. The abutment was manufactured with a constant size for all single-root 3D-printed implants. (b) Side view of a double-root 3D-printed implant. The abutment was manufactured with a constant size for all double-root 3D-printed implants. (c) Top view of a single-root 3D-printed implant. (d) Top view of a double-root 3D-printed implant. (e) Side view of a protective cap. (f) Side view of a protective cap. The number indicates the animal identification, and the letter indicates the location, distinguishing right (R) and left (L).

Figure 2. Clinical and radiographic photograph of single- and double-root 3D-printed implant

All protective caps were removed 2 weeks after implant placement for plaque control and implant stability measurements. There were no clinical signs of peri-implant inflammation, including redness, spontaneous bleeding, swelling, or ulceration. The clinical and radiographic photos were taken at the time of implant placement and 2,4,6,8,10,12 weeks after implant placement.

Figure 3. Implant stability test (IST) values of single- and double-root 3D-printed implants.

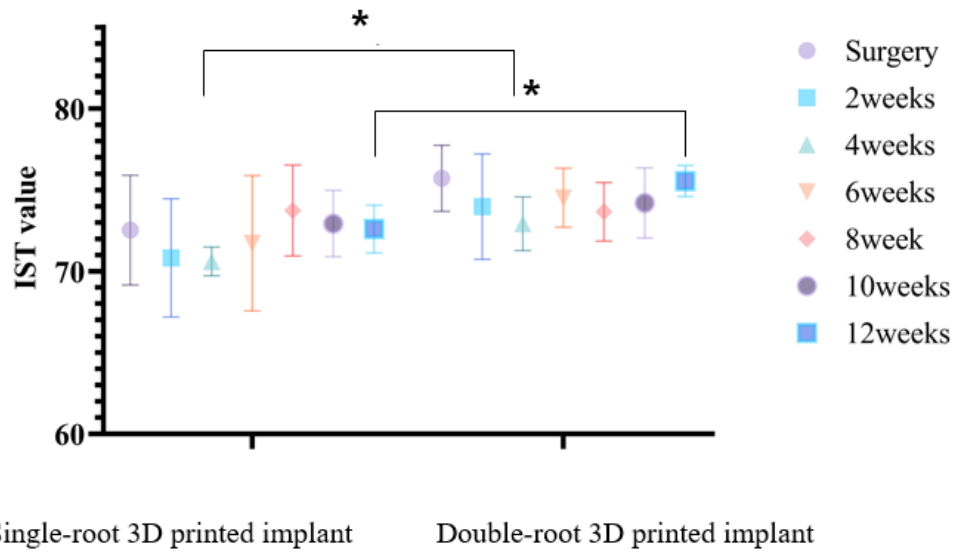

There were no significant difference in the stability value between single-root 3D-printed implants and double-root 3D-printed implants at each time point, except at 4 and 12 weeks, as shown by Sidak's double comparison test. There were no significant differences within the single-root 3D-printed implants and double-root 3D-printed implants throughout 12 weeks (p=0.0143, p=0.0320).

Figure 4. Radiographic changes in single- and double-root 3D-printed implant at 6 and 12 weeks

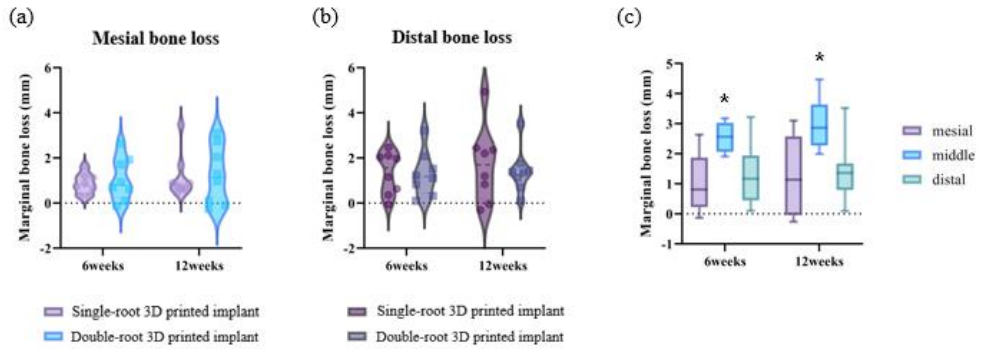

Radiographic changes (a) mesial bone loss in single- and double-root 3D-printed implant at 6 and 12 weeks (b) distal bone loss in single- and double-root 3D-printed implant at 6 and 12 weeks (c) Mesial, middle, and distal bone loss in double-root 3D-printed implant at 6 and 12 weeks. Asterisks (*) indicate statistically significant difference in marginal bone loss in the middle area compared with mesial and distal areas at 6 weeks and 12 weeks.

Figure 5. Representative micro-computed tomography (a) and analysis (b,c).

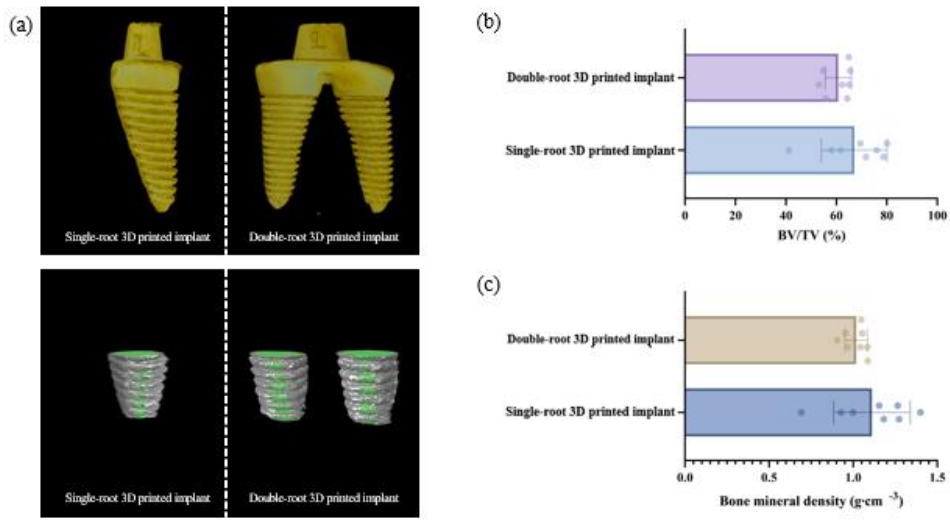

(a) Gray and green areas indicate the VOI and 3D-printed implants, respectively. BMD and BV/TV were measured in the gray area. (b) The BV/TV of single-root and double-root 3D-printed implant were 67.11±13.05% and 60.76±5.43%, respectively, showing no statistically significant difference. (c) The BMD of single-root and double-root 3D-printed implant were 1.11±0.23g·mm-3 and 1.02±0.08 g·mm-3, respectively, showing no statistically significant difference.

CT: computed tomography, VOI: volume of interest, BMD: bone mineral density, BV/TV: bone volume/tissue volume.

Figure 6. Representative of histologic view (a,b) and analysis (b,d).

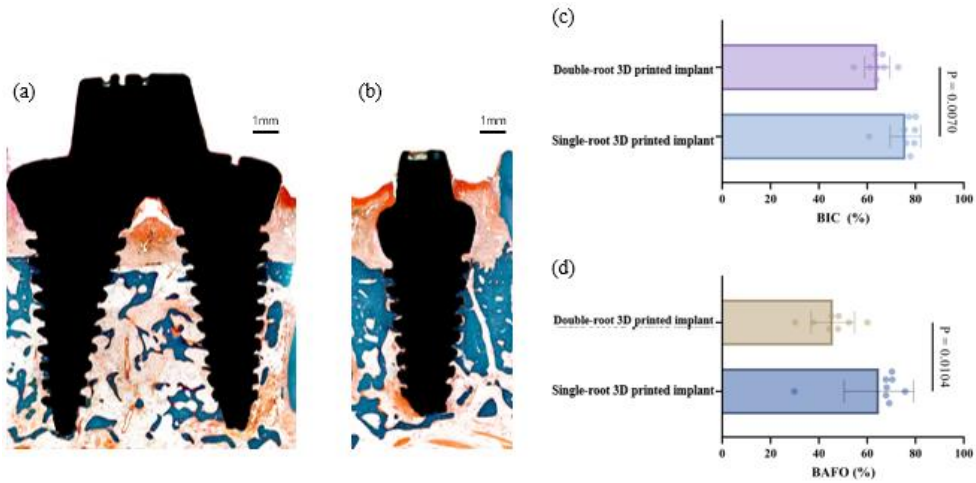

(a) Histomorphometric view of a double-root 3D-printed implant. Note the bone resorption in the furcation area. (b) Histomorphometric view of single-root 3D-printed implant (c) The BIC in single-root and double-root 3D-printed implants had statistically significant difference (75.87%±6.32% and 64.18±5.23%, respectively, p=0.0070) (d) The BAFO was statistically significantly different (p=0.0104) in single-root and double-root 3D-printed implants (64.88±14.37% and 45.81±9.01%, respectively)

BIC: bone-to-implant contact, BAFO: bone area fraction occupancy

Reference

1. Yu, N. *et al.* Estimation and change of edentulism among the Korean population: Korea National Health and Nutrition Examination Survey 2007–2018. *Epidemiol. Health.* **43**, e2021020 (2021).

2. Buser, D. *et al.* 10-year survival and success rates of 511 titanium implants with a sandblasted and acid-etched surface: A retrospective study in 303 partially edentulous patients. *Clin. Implant Dent. Relat. Res.* **14**(6), 839–851 (2012).

3. Degidi, M. *et al.* 10-year follow-up of immediately loaded implants with TiUnite porous anodized surface. *Clin. Implant Dent. Relat. Res.* **14**(6), 828–838 (2012).

4. Fischer, K. & Stenberg, T. Prospective 10-year cohort study based on a randomized controlled trial (RCT) on implant-supported full-arch maxillary prostheses. Part 1: Sandblasted and acid-etched implants and mucosal tissue. *Clin. Implant Dent. Relat. Res.* **14**(6), 808–815 (2012).

5. Zhang, X. *et al.* Long-term outcomes of early loading of straumann implant-supported fixed segmented bridgeworks in Edentulous Maxillae: A 10-year prospective study. *Clin. Implant Dent. Relat. Res.* **18**(6), 1227–1237 (2016).

6. Hodosh, M. *et al.* The dental polymer implant concept. *J. Prosthet. Dent.* **22**(3), 371–380 (1969).

7. Lee, J. *et al.* A narrative review of contemporary evaluation methods for root analog implants. *J. Implantol. Appl. Sci.* **26**(1), 51–72 (2022).

8. Mangano F. *et al.* Custom-made, root-analogue direct laser metal forming implant: a case report. *Lasers Med. Sci.* **27**, 1241–1245 (2012).

9. Dantas T. *et al.* Customized Root-Analogue Implants: A Review on Outcomes from Clinical Trials and Case Reports. *Mater.* **14**(9), 2296 (2021).

10. Pirker W. & Kocher A. Immediate, non-submerged, root-analogue zirconia implants placed into single-rooted extraction sockets: 2-year follow-up of a clinical study. *Int. J. Oral Maxillofac. Surg.* **38**, 1127–1132 (2009).

11. Figliuzzi M. & Mangano F. A novel root analogue dental implant using CT scan and CAD/CAM: Selective laser melting technology. *Int. J. Oral Maxillofac. Surg.* **41**, 858-862 (2012).

12. Mangano F. *et al.* Immediate, non-submerged, root-analogue direct laser metal sintering (DLMS) implants: A 1-year prospective study on 15 patients. *Lasers Med. Sci.* **29**, 1321-1328 (2014).

13. Moin D. *et al.* Immediate Nonsubmerged Custom Root Analog Implants: A Prospective Pilot Clinical Study. *Int. J. Oral Maxillofac. Implant* **33**, e37–e44 (2018).

14. Böse M. *et al.* Clinical Outcomes of Root-Analogue Implants Restored with Single Crowns or Fixed Dental Prostheses: A Retrospective Case Series. *J. Clin. Med.* **9**(8), 2346 (2020).

15. Tack, P. *et al.* 3D-printing techniques in a medical setting: a systematic literature review. *Biomed. Eng. Online* **15**(1), 115 (2016).

16. Lin, L. *et al.* 3D printing and digital processing techniques in dentistry: A review of literature. *Adv. Eng. Mater.* **21**(6), 1801013 (2019).

17. Moin, D. *et al.* Designing a novel dental root analogue implant using cone beam computed tomography and CAD/CAM technology. *Clin. Oral Implants Res.* **24 Suppl A100**, 25–27 (2013).

18. Li, L. *et al.* Comparison of 3D-printed dental implants with threaded implants for osseointegration: An experimental pilot study. *Materials (Basel)* **13**(21), 4815 (2020).
19. Lee, J. *et al.* The impact of surface treatment in 3-dimensional printed implants for early osseointegration: A comparison study of three different surfaces. *Sci. Rep.* **11**(1), 10453 (2021).
20. Ren, B. *et al.* Improved osseointegration of 3D printed Ti-6Al-4V implant with a hierarchical micro/nano surface topography: An in vitro and in vivo study. *Mater. Sci. Eng. C.* **118**, 111505 (2021).
21. Kim, J. *et al.* Mechanophysical and biological properties of a 3D-printed titanium alloy for dental applications. *Dent. Mater.* **36**(7), 945–958 (2020).
22. Tunchel, S. *et al.* 3D printing/additive manufacturing single titanium dental implants: a prospective multicenter study with 3 years of follow-up. *Int. Dent. J.* **2016**, 9 (2016).
23. Shah, F. *et al.* Commercially pure titanium (cp-Ti) versus titanium alloy (Ti6Al4V) materials as bone anchored implants — Is one truly better than the other?, *Mater. Sci. Eng. C.* **62,** 960-966 (2016).
24. Traini, T. *et al.* Direct laser metal sintering as a new approach to fabrication of an isoelastic functionally graded material for manufacture of porous titanium dental implants. *Dent. Mater.* **24**(11), 1525–1533 (2008).
25. Aufa, A. *et al.* Recent advances in Ti-6Al-4V additively manufactured by selective laser melting for biomedical implants: prospect development. *J. Alloys Compd.* **896**, 163072 (2022).
26. Chandar S. *et al.* In vitro evaluation of cytotoxicity and

corrosion behavior of commercially pure titanium and Ti-6Al-4V alloy for dental implants, *J. Indian Prosthodont. Soc.* **17**(1):35-40 (2017).

27. Suresh S. *et al.* Mechanical properties and in vitro cytocompatibility of dense and porous Ti–6Al–4V ELI manufactured by selective laser melting technology for biomedical applications, *J Mech. Behav. Biomed. Mater*. **123**, 104712 (2021).

28. Sánchez-López J. *et al.* Ti6Al4V coatings on titanium samples by sputtering techniques: Microstructural and mechanical characterization, *J. Alloys Compd.* **952** (2023).

29. Shaoki, A. *et al.* Osseointegration of three-dimensional designed titanium implants manufactured by selective laser melting. *Biofabrication* **8**(4), 045014 (2016).

30. Hong, D. and Oh, J. Recent advances in dental implants. *Maxillofac. Plast. Reconstr. Surg.* **39**(33), (2017).

31. Lee, J. *et al.* Impact of lattice versus solid structure of 3D-printed multiroot dental implants using Ti-6Al-4V: a preclinical pilot study. *J. Periodontal Implant Sci.* **52**(4), 338-350 (2022).

32. Walter, C. *et al.* Periodontal surgery in furcation-involved maxillary molars revisited—An introduction of guidelines for comprehensive treatment. *Clin. Oral Investig.* **15**(1), 9–20 (2011).

33. Pramanik, A. Problems and solutions in machining of titanium alloys. *Int. J. Adv. Manuf. Technol.* **70**, 919-928 (2014).

34. Murr, L. Microstructure and mechanical behavior of Ti-6Al-4V produced by rapid-layer manufacturing, for biomedical applications. *J. Mech. Behav. Biomed. Mater.* **2**, 20-32 (2009).

35. Nguyen H. *et al.* A critical review on additive manufacturing of Ti-6Al-4V alloy: microstructure and mechanical properties, *J. Mater. Res. Technol.* **18**, 4641-4661 (2022).

36. Gibson I., *et al. Additive manufacturing technologies.* Vol. 17. Cham, Switzerland: *Springer* (2021).

37. Kim, H. *et al.* A resonance frequency analysis of sandblasted and acid-etched implants with different diameters: A prospective clinical study during the initial healing period. *J. Periodontal Implant Sci.* **47**(2), 106–115 (2017).

38. Ramanauskaite, A. *et al.* A systematic review on the influence of the horizontal distance between two adjacent implants inserted in the anterior maxilla on the inter-implant mucosa fill. *Clin. Oral Implants Res.* **29**(Suppl 15), 62–70 (2018).

39. Danza, M. *et al.* Distance between implants has a potential impact of crestal bone resorption. *Saudi Dent. J.* **23**(3), 129-133 (2011)

40. Schwarz, F. *et al.* Peri-implantitis. *J. Clin. Periodontol.* **45**(Suppl 20), S246– S266 (2018).

41. Ragucci, G. *et al.* Immediate implant placement in molar extraction sockets: A systematic review and meta-analysis. *Int. J. Implant Dent.* **6**(1), 40 (2020).

국문초록

Ti-6Al-4V로 제작한 단근과 다근 3D-프린트 임플란트의 전임상 비교연구

정 인 나

서울대학교 대학원

치의과학과 치주과학 전공

(지도교수 구 기 태)

1. 연구목적

본 연구의 목적은 단근 및 다근 3D-프린트 임플란트를 마이크로 컴퓨터 단층 촬영(micro-CT) 및 조직학적 분석을 통해 비교하고자 하였다.

2. 연구방법

4마리의 비글견의 하악 제3소구치와 제4소구치에 3D -프린트 단근 및 다근 임플란트를 제작하여 식립하였다. 각 그룹에 8개의 임플란트를 발치 직후 식립하였다. 감쇠능를 측정하였고 치근단촬영은 12주 동안 2주 간격으로 촬영하였다. 임플란트 주변의 골면적비율/조직면적비율

(BV/TV) 및 골밀도(BMD)를 micro-CT로 측정하였다. 골-임플란트 접촉 길이(BIC) 및 골면적부분 점유율(BAFO)는 조직학적 샘플에서 측정되었다.

3. 결 과

모든 단일 및 다근 3D-프린트 임플란트는 임플란트 주위염의 임상 징후 없이 생존하였다. 그룹 간의 임플란트 안정성 값은 4주와 12주를 제외하고는 통계적으로 차이가 없었다. 변연골 변화는 다근 임플란트의 중간 부위를 제외하고 근심부와 원위부에서 그룹 간의 통계적인 차이가 없는 것으로 관찰되었다. 다근 3D-프린트 임플란트의 BV/TV 및 BMD는 micro-CT 분석에서 단근 3D-프린트 임플란트에 비해 통계적으로 유의미한 차이를 보이지 않았지만, 조직 형태 분석에서 BIC 및 BAFO 값이 낮았다.

4. 결 론

단근 3D-프린트 임플란트와 비교하여 다근 3D-프린트 임플란트는 고정체 주변에서 유사한 안정성과 골재형성이 나타나지만, 이개부 영역에서 통계적으로 유의미한 변연골 손실은 여전히 문제가 있다.

주요어 : 치과용 임플란트, 골유착, 3D 프린팅

학 번 : 2020-39210